[CANCER RESEARCH 64, 3209–3214, May 1, 2004]

Endothelin-1 Is a Critical Mediator of Myogenic Tone in Tumor Arterioles: Implications for Cancer Treatment

Pierre Sonveaux,[1] Chantal Dessy,[1] Philippe Martinive,[1] Xavier Havaux,[2] Bénédicte F. Jordan,[3] Bernard Gallez,[3] Vincent Grégoire,[4] Jean-Luc Balligand,[1] and Olivier Feron[1]

[1]University of Louvain Medical School, Unit of Pharmacology and Therapeutics (FATH 5349); [2]Cardiovascular Pathology Unit; [3]Biomedical Magnetic Resonance Unit and Medicinal Chemistry and Radiopharmacy Unit; and [4]Radiobiology and Radioprotection Unit, Brussels, Belgium

ABSTRACT

Although derived from the host tissue, the tumor vasculature is under the influence of the tumor microenvironment and needs to adapt to the resistance to blood flow inherent to the dynamics of tumor growth. Such vascular remodeling can offer selective targets to pharmacologically modulate tumor perfusion and thereby improve the efficacy of conventional anticancer treatments. Radiotherapy and chemotherapy can, indeed, take advantage of a better tumor oxygenation and drug delivery, respectively, both partly dependent on the tumor blood supply.

Here, we showed that isolated tumor arterioles mounted in a pressure myograph have the ability, contrary to size-matched healthy arterioles, to contract in response to a transluminal pressure increase. This myogenic tone was exquisitely dependent on the endothelin-1 pathway because it was completely abolished by the selective endothelin receptor A (ET_A) antagonist BQ123. This selectivity was additionally supported by the large increase in endothelin-1 abundance in tumors and the higher density of the ET_A receptors in tumor vessels. We also documented by using laser Doppler microprobes and imaging that administration of the ET_A antagonist led to a significant increase in tumor blood flow, whereas the perfusion in control healthy tissue was not altered. Finally, we provided evidence that acute administration of the ET_A antagonist could significantly stimulate tumor oxygenation, as determined by electron paramagnetic resonance oximetry, and increase the efficacy of low-dose, clinically relevant fractionated radiotherapy.

Thus, blocking the tumor-selective increase in the vascular endothelin-1/ET_A pathway led us to unravel an important reserve of vasorelaxation that can be exploited to selectively increase tumor response to radiotherapy.

INTRODUCTION

The tumor vasculature has unique features, which may be viewed as many selective targets for anticancer strategies. Accordingly, the last 15 years have witnessed the development of drugs targeting tumor vessels, namely the antiangiogenic (1, 2) and antivascular agents (3). Although the goals of these approaches are different (*e.g.,* to prevent new blood vessel formation and to occlude/destroy pre-existing vessels, respectively), they both exploit the specific phenotype of endothelial cells lining tumor blood vessels to selectively target tumor perfusion (4). An interest also simultaneously developed for opposite strategies aiming to enhance the tumor perfusion (5, 6). The rationale for such qualitative improvement in the function of tumor blood vessels is to increase the efficacy of radio- or chemotherapy (7, 8). This concept implies that the effects on tumor blood flow need to be transient and selective. Although the action of vasomodulatory drugs can be controlled by adapting their protocol of administration, the selectivity issue is limiting and matter of investigation (9).

We and others have reported that drugs like nitric oxide donors (10, 11), nicotinamide (12), bradykinin agonist (13), and insulin (14), but also radiations and chemotherapeutic agents themselves (15–17), could modulate tumor blood flow, oxygenation, and permeability, thereby optimizing associated antitumor treatments. The validity of these adjuvant approaches to conventional chemo- and radiotherapy was usually verified *a posteriori* by documenting a better tumor response with very limited insights on the mechanisms of the tumor selectivity. Conversely, studies that did not look for a gain in treatment efficacy have identified the existence of tumor-specific vascular reactivity to various products including endothelin (18), endothelin agonist (19), angiotensin (20, 21), noradrenaline (22), hemoglobin A (23), and tumor necrosis factor α (24).

We reasoned that the identification of vasomodulatory pathways truly selective of the tumor vasculature could arise from the *ex vivo* comparison of the intrinsic pharmacological reactivity of vessels issued either from tumors or from the tumor-hosting tissues. Indeed, the variety of chemokines and cytokines released by tumor cells are known to trigger regulatory processes within the tumor vasculature leading to phenotypic shift including escape from immunosurveillance and adaptation to hypoxia (2, 25, 26). Therefore, it was very likely that the tumor microenvironment could also, directly or indirectly, induce profound alterations in the tumor vessel reactivity. Accordingly, using a myograph (originally dedicated to study the physiopathology of normal arterioles), we reported recently that the acetylcholine-induced nitric oxide-mediated vasodilation was dramatically altered in tumor arterioles (15). Also, in the same study, we documented how ionizing radiations by reversing the lack of NO-mediated response of tumor vessels could increase the sensitivity of the tumor to further X-ray fractions (15).

In the current study, our reflection started from the growing evidence that endothelin-1 production is increased in many tumor types where it plays crucial roles in proliferation and angiogenesis (27–29). In these studies, however, there was no mention of the powerful vasoconstrictive effects of endothelin-1 (ET-1) and its potential action on the contractile tone of tumor vessels. Indeed, although ET-1 can induce vasodilation through activation of the endothelin receptor B (ET_B), a powerful vasoconstriction is obtained when ET-1 interacts with the endothelin receptors A and B (ET_A and ET_B) located on smooth muscle cells. In this study, we therefore asked ourselves whether the tumor production of ET-1 could influence local vascular tone and whether blocking ET-1 signaling could have an impact on tumor blood flow and thereby be exploited to promote conventional antitumor therapy.

MATERIALS AND METHODS

Mice. NMRI, C57BL/6J, and C3H/He male mice (Elevage Janvier, Le Genest-St-Isle, France) were used in experiments with transplantable liver tumor (TLT; mouse hepatocarcinoma; Ref. 30), Lewis Lung carcinoma (mouse lung carcinoma; Ref. 31), and Fibrosarcoma-II (mouse fibrosarcoma; Ref. 32) syngeneic tumor cells, respectively. Anesthetized mice (ketamine/xylazine) received i.m. injections of 10^5-10^6 tumor cells in the vicinity of the saphenous arteriole of the posterior right leg. The pre-existing arteriole was progressively co-opted as the

Received 5/8/03; revised 2/18/04; accepted 2/26/04.

Grant support: Fonds de la Recherche Scientifique Médicale, the Belgian Federation Against Cancer, the Fortis Cancerology Research Fund, the J. Maisin Foundation, and the Association Sportive Contre le Cancer. C. Dessy and O. Feron are FNRS (Fonds National de la Recherche Scientifique) Research Associates. P. Sonveaux and B. F. Jordan are FNRS Research Assistants.

Note: P. Sonveaux and C. Dessy contributed equally to this work.

The costs of publication of this article were defrayed in part by the payment of page charges. This article must therefore be hereby marked *advertisement* in accordance with 18 U.S.C. Section 1734 solely to indicate this fact.

Requests for reprints: University of Louvain Medical School, Unit of Pharmacology and Therapeutics (FATH 5349), Brussels B-1200, Belgium. Phone: 32-2-764-5349; Fax: 32-2-764-9322; E-mail: feron@mint.ucl.ac.be.

tumor grew (see Fig. 1*G*). The tumor diameters were tracked with an electronic caliper. When the tumor diameter reached 4.0 ± 0.5 mm, mice were sacrificed or randomly assigned to a treatment group. When indicated, they received an i.p. injection of the selective ET_A antagonist BQ123 (0.5, 1, and 2 mg/kg; Sigma, Bornem, Belgium) or saline alone. Each procedure was approved by the local authorities according to national animal care regulations.

Immunoblottings and Immunostainings. Immunoblottings were carried out, as described previously (15, 33), with a sheep polyclonal antibody against ET_A (Abcam, Cambridge, United Kingdom) or ET_B (Alomone Labs, Jerusalem, Israel). For immunostainings, collected tissue samples were cryosliced and probed with a rabbit polyclonal antibody against ET-1 (gift from Ronald van Beneden, University of Louvain, Brussels, Belgium; Ref. 34). Endogenous peroxidase activity was inhibited by 0.3% H_2O_2 in PBS, and Envision system (Dako, Glostrup, Denmark) was used for revelation. Sections were finally counterstained with Mayer's hematoxylin. Quantitative image analyses of immunostained arteriole slices (5 arterioles/condition and 3 sections/animal) were performed with AnalySIS software (Soft Imaging System, Münster, Germany).

Myograph Assays. Tumor saphenous arterioles and size-matched arterioles from healthy mice were dissected under a stereoscopic microscope and mounted on a 110P pressure myograph (DMT, Aarhus, Denmark). No macroscopic differences were detectable between the tumor and control arterioles (diameters of 284 ± 14 and 299 ± 17 μm, respectively; $P > 0.1$). Changes in the outer diameters were tracked and measured with the Myoview software (DMT). To evaluate the myogenic tone, isolated arterioles were left to recover for 45–60 min in no-flow condition (20 mm Hg; 37.5°C). Then, the pressure was increased by steps of 20 mm Hg (that were maintained for 15 min to allow arteriole response). For each pressure step, the active vessel diameter was determined in physiological salt solution buffer (NaCl 119 mM, KCl 4.7 mM, $NaHCO_3$ 25 mM, KH_2PO_4 1.18 mM, $MgSO_4$ 1.17 mM, EDTA 0.026 mM, glucose 5.5 mM, and $CaCl_2$ 1.6 mM); then the passive diameter of the same arteriole was measured in $CaCl_2$-deprived physiological salt solution supplemented with 10 μM sodium nitroprusside and 2 mM EGTA. In some experiments, the active diameter was determined after a 60-min preincubation in the calcium-containing physiological salt solution buffer with BQ123 (1 μM).

For the establishment of the ET-1 dose-response curve, isolated arterioles were left to recover at physiological pressure for 45–60 min in no-flow condition in physiological salt solution medium (60 mm Hg, 37.5°C); additive doses of ET-1 (Sigma) were then delivered in the bathing medium. For each vessel used in this study, the ability of the vessels to contract upon application of a depolarizing KCl solution was verified at the end of the experiment and compared with a similar contraction performed at the very beginning of the experiment. If these two contractions differed by >10%, the experiment was disregarded.

Tumor Blood Flow Monitoring. Tumor perfusion was measured with a Laser Doppler imager (Moor Instruments) and with Laser Doppler microprobes (Oxyflo; Oxford Optronix). Briefly, for the Laser Doppler imaging measurements, mice were anesthetized and fur was removed from the limbs using a depilatory cream. They were placed on a heating pad (37°C) to minimize variations in temperature. The average perfusions of the tumor-bearing leg and of the control leg were evaluated on the basis of colored histogram pixels. For the Oxyflo measurements, fiber-optic microprobes (Laser Doppler + thermocouple) were introduced into the tumor. Back scattering measurements were used to validate the absence of movement artifacts. A 10-min baseline of stable recordings was obtained before treatment administration through the catheterized tail vein; data were collected continuously at a sampling frequency of 20 Hz.

Electron Paramagnetic Resonance (EPR) Oximetry. This real-time, O_2-nonconsuming technique was used to track the changes in pO_2 induced by BQ123 administration. EPR oximetry relies on the oxygen-dependent broadening of the EPR linewidth of a paramagnetic oxygen sensor preimplanted in the tumor. Accordingly, 50 μl of a suspension (100 mg/ml) of the O_2-sensitive probe (charcoal wood powder, CX0670–1; EM Science, Gibbstown, NJ) were injected in the center of the tumor 24 h before X-ray irradiation, as described previously and validated (10, 14, 15). The tumors of anesthetized mice were placed in the center of the surface coil. EPR spectra were recorded using an

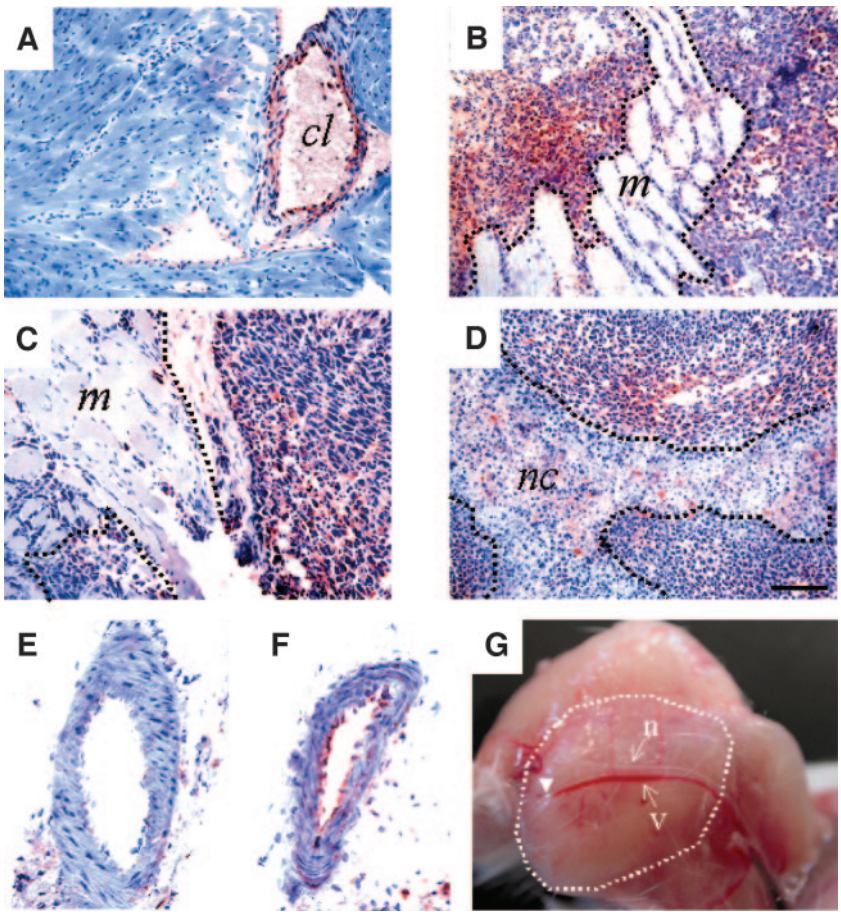

Fig. 1. Immunodetection of endothelin-1 (ET-1) in tumor and tumor vessels. ET-1 antibodies were used to immunostain (*A*) cardiac tissue from healthy mice (*cl* indicates the lumen of a coronary artery); (*B*) transplantable liver tumor; (*C*) Lewis Lung carcinoma tumor; and (*D*) Fibrosarcoma-II tumor. ---- delineate the healthy muscular tissue (*m*) surrounding tumors or the central necrotic core (*nc*). *Bar* = 100 μm. Saphenous arterioles from (*E*) healthy or (*F*) tumor-bearing mice were also immunostained for ET-1 expression. *G,* shown is the anatomical location of the saphenous arteriole located between the saphenous vein (*v*) and nerve (*n*); the ---- shows the limits of the tumor and the *arrowhead* indicates where the arteriole enters the tumor (*e.g.,* where arterial segments were isolated for myograph studies).

EPR spectrometer (Magnettech, Berlin, Germany) with a low frequency microwave bridge operating at 1.1 GHz and extended loop resonator.

Radiotherapy and Tumor Measurements. Anesthetized TLT tumor-bearing mice were irradiated using the RT-250 device (Philips) for a dose delivery of 0.76 Gy/min. Mice were shielded with lead except for a 3-cm-diameter circular field where the tumor was centered. When indicated, mice received an i.p. injection of 1 mg/kg BQ123 or saline alone, 45-min before each dose delivery. Tumor-bearing and control legs were daily measured with an electronic caliper, the difference corresponding to the tumor diameter. Mean regrowth delays refer to the doubling of the tumor diameters.

Statistical Analyses. Data are reported as mean ± SE; Student's *t* test or two way ANOVA were used where appropriate. To determine synergism, we compared tumor doubling times using a nonparametric Mann-Whitney analysis; a generalized linear model with two-way ANOVA was also applied and led to similar results.

RESULTS

Expression of ET-1 in Tumor Cells and in the Tumor Vasculature. We first characterized the ET-1 production in 3 syngeneic tumor models (TLT, Lewis Lung carcinoma, and Fibrosarcoma-II) obtained by i.m. injections of tumor cells. When reaching a diameter of 4.0 ± 0.5 mm, the tumors were resected and processed for immunostaining with ET-1 antibodies; mouse heart was used as control for antibody specificity (see Fig. 1*A*). As shown in Fig. 1, *B–D,* the different tumors were found to produce large amounts of ET-1 that were detectable both inside the tumor cells and in the extracellular space. Very low amounts of ET-1 were found in the healthy surrounding muscular tissues (see Fig. 1, *B* and *C*) and in the necrotic core of the tumor (see Fig. 1*D*). Importantly, the co-opted tumor vasculature was strongly labeled, revealing a 13-fold increase ($P < 0.05$; $n = 15$) in ET-1 in the vessel wall when compared with control size-matched arterioles (Fig. 1, *E* and *F*).

Differential Reactivity of Tumor Arterioles to ET-1. To evaluate the vasomodulatory effects of the increased ET-1 concentrations in tumor arterioles, we isolated TLT-co-opted arterioles (see Fig. 1*G*) and size-matched arterioles from healthy animals. These arterioles were mounted on a pressure myograph, and after pressurization and equilibration, exposed to increasing doses of ET-1. In arterioles from healthy mice, low ET-1 concentrations (10^{-13}-10^{-10} M) were ineffective, whereas higher doses (10^{-9}-10^{-7} M) dose-dependently constricted the vessels (Fig. 2*A*). By contrast, tumor-co-opted arterioles contracted with ET-1 concentrations as low as 10^{-11} M (Fig. 2*A*) and reached a maximum at 10^{-8} M ET-1 (the maximum contraction was obtained at 10^{-7} M ET-1 in control vessels). Calculated EC_{50}s were 0.40 nM and 2.01 nM ($P < 0.05$; $n = 5$) in tumor and in size-matched healthy arterioles, respectively. Immunoblots performed on carefully microdissected arterioles (cleaned from surrounding tissues) also revealed that the density of ET_A (*e.g.,* the ET-1 receptor mediating vasoconstriction) was increased by 5-fold in co-opted vessels *versus* healthy arterioles (Fig. 2*B*). Interestingly, when using total lysates from tumors, we failed to detect ET_A receptor by immunoblotting suggesting a weaker density of this receptor in tumor cells than in vascular cells.

The density of ET_B receptors was not significantly altered in co-opted tumor arterioles (Fig. 2*B*), and immunohistochemistry revealed that most of the ET_B signal was concentrated in the endothelial layer of the arterioles (data not shown).

Tumor Arterioles Exhibit a Myogenic Tone Sensitive to an ET_A Antagonist. Because we have identified that tumor arterioles are chronically exposed to large amounts of ET-1 (see Fig. 1) and are (remain) hyper-responsive to ET-1 (see Fig. 2), we next examined whether intrinsic features of tumor arterioles were under the tonic control of this pathway. Accordingly, we examined the presence in tumor arterioles of a differential myogenic tone (*i.e.,* the ability of arterioles to contract when the intraluminal pressure increases; Ref. 35). Myogenic vasoconstriction is, indeed, thought to provide a level of basal tone that enables arterioles to respond to neurohumoral stimuli with the appropriate changes in vessel diameter.

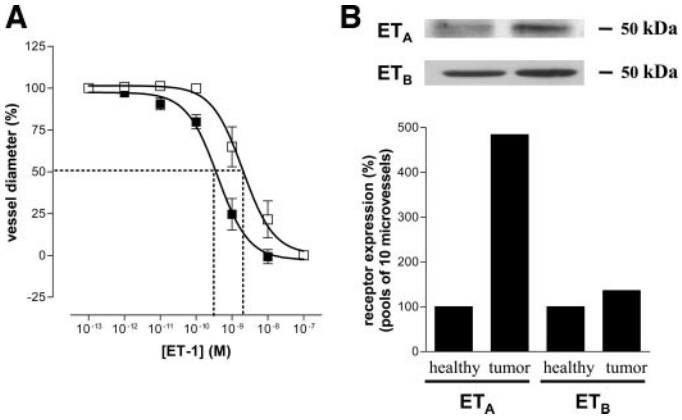

Fig. 2. Tumor arterioles are hyper-responsive to endothelin-1 (*ET-1*) and overexpress smooth muscle endothelin receptor A (ET_A) receptor. *A,* arterioles isolated from healthy (□) and from transplantable liver tumor-bearing mice (■) were mounted on a pressure myograph and exposed to increasing doses of ET-1. Results are expressed as percentage of the maximal contraction obtained with 10^{-7} M ET-1. Sigmoidal fitting shows that the dose/effect curves for healthy and tumor vessels ($R^2 = 0.91$ and 0.98, respectively) were significantly different ($P < 0.01$; $n = 5$); note that some SE are smaller than symbols; *bars,* ±SE. *B,* pools of arterioles from healthy and transplantable liver tumor-bearing mice were lysed (to obtain enough material) and were immunoblotted with endothelin receptor A (ET_A) and endothelin receptor B (ET_B) antibodies. Shown are representative immunoblots and a bar graph depicting the densitometric analysis of two different immunoblots (2 pools of 10 arterioles/condition).

Using a pressure myograph, we examined the response of isolated tumor-co-opted and control arterioles to step-by-step increases of the luminal pressure. Accordingly, the changes in the active diameter (measured in calcium-containing medium) and in the passive diameter (determined in a medium devoid of calcium) were consecutively tracked for each arteriole. In healthy mice, no myogenic tone was observed: both the active and the passive diameters increased similarly when the pressure raised (Fig. 3*A*). By contrast, tumor-co-opted arterioles were able to respond to the pressure increase by a vasoconstriction (detected as a lesser vasodilation) in calcium-containing, but not in calcium-deprived medium (Fig. 3*B*), thereby acknowledging the existence of an intrinsic myogenic tone.

We then investigated the implication of the ET-1/ET_A pathway in the myogenic tone of TLT tumor-co-opted arterioles by using the specific ET_A antagonist BQ123. The effect of the preincubation with BQ123 was dramatic, because it completely abrogated the myogenic tone (Fig. 3*B; P* < 0.01). In fact, the active diameter curve under ET_A inhibition (Fig. 3*B, black triangles*) was not different from the passive diameter curve (Fig. 3*B, open circles*). As a control, we also demonstrated that ET_A inhibition left unaffected the active diameter of size-matched arterioles from healthy mice (Fig. 3*A*).

ET_A Inhibition Triggers a Tumor-Specific Increase in Blood Flow and Oxygenation. We then investigated whether the BQ123-mediated abrogation of the myogenic tone (as elicited *ex vivo*) was correlated with an increased tumor perfusion *in vivo*. Accordingly, TLT tumor-bearing mice received a bolus i.p. injection of 1 mg/kg BQ123 or saline, and the perfusion of both the tumor-bearing and the control legs was monitored using a Laser Doppler imaging system. In BQ123-treated mice, we consistently observed an important increase in the blood flow of the tumor-bearing leg (Fig. 4*A, top panel, white circle*), whereas the healthy opposite leg failed to show any significant changes in perfusion (Fig. 4*A, top panel, white arrows*). Importantly, isovolemic saline i.p. injection barely increased the basal perfusion in the tumor-bearing leg (see Fig. 4*A, lower panels*, and Fig. 4*B*). We also used Laser Doppler needle probes directly introduced in the tumors to validate the results

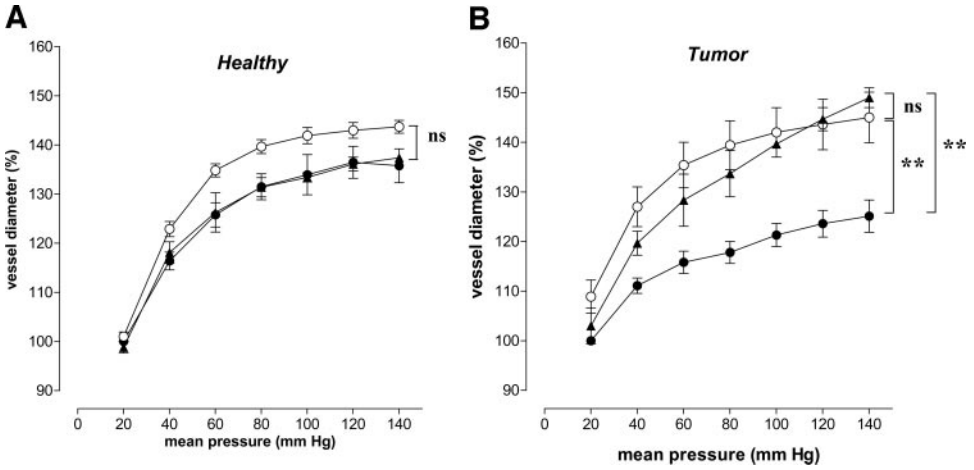

Fig. 3. Tumor arterioles exhibit an endothelin receptor A-dependent myogenic tone. Isolated arterioles were mounted on a pressure myograph and allowed to respond to a step-by-step increase of the luminal pressure. Changes in vessel diameter were tracked in bathing media containing calcium (active diameter, ●; $n = 10$) or not (passive diameter, ○; $n = 10$). Saphenous arterioles were dissected from healthy mice (*A*) or were isolated from transplantable liver tumor (after co-option; *B*). In some experiments, arterioles were preincubated with the endothelin receptor A antagonist BQ123 (1 μM) in the calcium-containing medium (active diameter, ▲; $n = 3$); *ns,* not significantly different; **, $P < 0.01$ between the indicated dose/effect curves); *bars,* ±SD.

obtained with the imager. A similar increase in blood flow was observed after BQ123 administration (Fig. 4*C*).

Using EPR oximetry, we also evaluated the BQ123-induced changes in tumor pO_2. Fig. 4*D* shows that 60 min after administration of the ET_A antagonist (but not of the saline solution), the tumor oxygenation was significantly increased over basal level (+174%; $P < 0.01$; $n = 7$). Of note, the measured pO_2 corresponds to the mean value in a tumor volume of ±10 mm^3 (*i.e.,* the volume of charcoal dispersion as determined by histology) and, therefore, does not preclude more dramatic variations in specific regions of the tumor.

ET_A Inhibition Radiosensitizes Tumors. In various tumor models, improved tumor perfusion is associated with a net increase in tumor oxygenation, which may be exploited to increase the effectiveness of radiotherapy (10, 14, 15). Therefore, we tested the hypothesis that ET_A inhibition could radiosensitize tumors. Accordingly, we daily determined the tumor diameters of mice receiving (or not) fractionated radiotherapy, and evaluated the effects of BQ123 administered 45 min before each radiation fraction (to have the maximum increase in pO_2 at the time of X-ray exposure; see Fig. 4). As shown in Fig. 5, *A* and *B,* and Table 1, when fractionated radiotherapy (5 × 2 Gy and 2 × 6 Gy) was combined to the BQ123 pretreatment, the overall benefit on tumor growth retardation was higher than the sum of the effects of the two treatments administered separately ($P < 0.01$; $n = 8–11$). Similar data were obtained with two other tumor models, namely Lewis Lung carcinoma tumors and Fibrosarcoma-II (data not shown); both tumor types overexpress ET-1 (see Fig. 1, *C* and *D*) and arterioles issued from the former were shown to also exhibit myogenic tone (data not shown).

A dose-response curve was also generated using three different doses of BQ123 (0.5, 1, and 2 mg/kg) in combination with the 2 × 6 Gy protocol (Fig. 5*C*). Although limitations in BQ123 availability precluded additional exploration, it is noteworthy that with the higher dose (2 mg/kg), two mice (of 6) were in remission 5 weeks after treatment (see Fig. 5 legend). Of note, at each dose used in this study, BQ123 (two or five i.p. injections) only slightly restrained tumor growth by itself (see Fig. 5, *A* and *B,* and Table 1).

DISCUSSION

The two major findings of this study are: (*a*) that basal production of ET-1 in tumors leads to the development of a myogenic tone that represents an important reserve for vasorelaxation; and (*b*) that the use

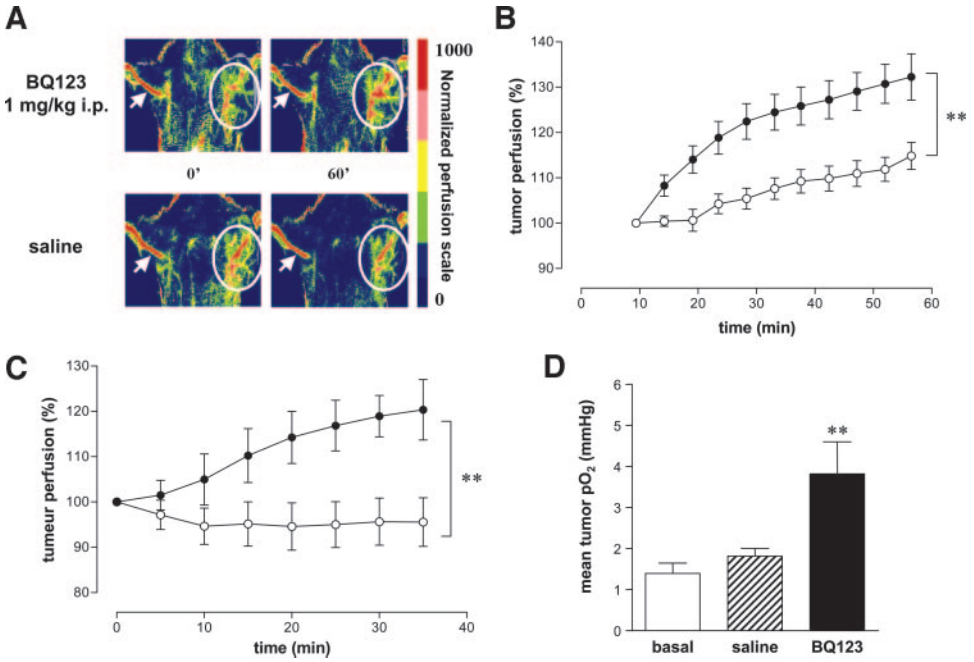

Fig. 4. Endothelin receptor A inhibition increases tumor blood flow and oxygenation. *A,* shown are typical Laser Doppler imaging pictures obtained before (time 0) and 60 min after i.p. injection of 1 mg/kg BQ123 (*top panels*) or vehicle alone (*bottom panels*). On each picture, the tumor-bearing leg is on the right (*white circle*) and the control leg on the left (*white arrow*). *B,* shown is the time course of global changes in tumor perfusion (derived from Laser Doppler imaging color pixel histograms) after BQ123 (●; $n = 11$) or saline (○; $n = 10$) injection; data are expressed as percentage of the basal perfusion. (**, $P < 0.01$ when comparing the two curves). *C,* shown is the time course of local changes in tumor perfusion determined with Laser Doppler needle microprobes (Oxyflo) after BQ123 (●) or saline (○) injection ($n = 12$). Data are expressed as percentage of the basal perfusion at time 0 (**, $P < 0.01$ when comparing the two curves). *D,* bar graph represents the tumor pO_2 measured by electron paramagnetic resonance at baseline (□; $n = 14$) and 45 min after saline (▨; $n = 7$) or BQ123 (■; $n = 7$) administration (**, $P < 0.01$); *bars,* ±SD.

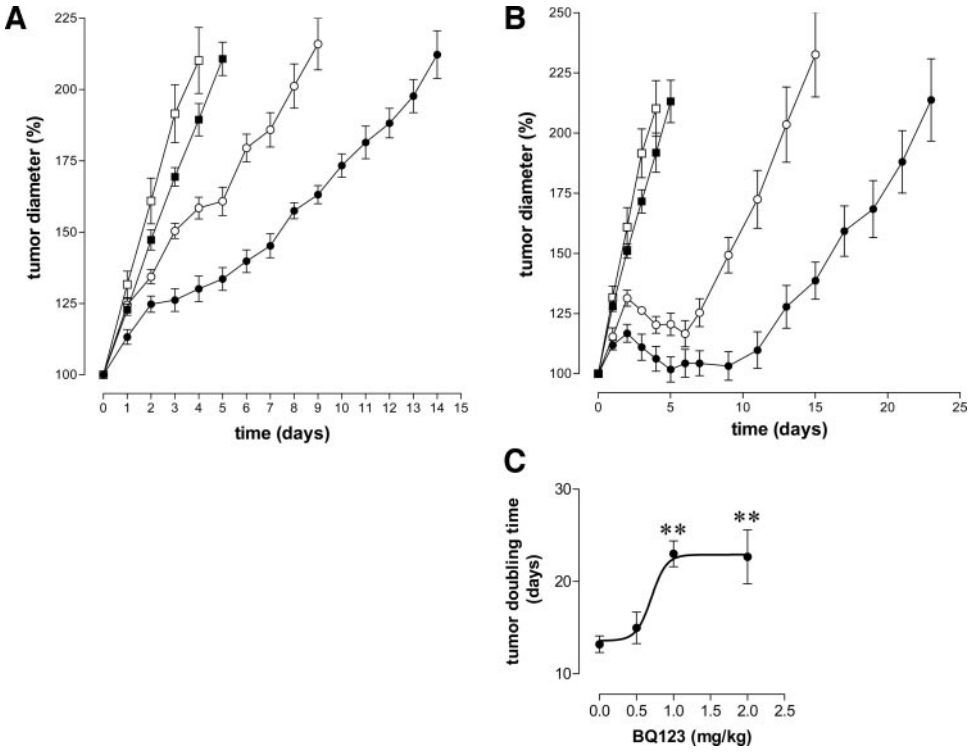

Fig. 5. Endothelin receptor A inhibition radiosensitizes tumors. Growth of transplantable liver tumors was determined by measuring tumor diameters in untreated mice (□), in mice treated with 1 mg/kg BQ123 alone (■), with irradiation and vehicle (○), and with the combination of irradiation and BQ123 (●). Irradiated mice received either (*A*) five fractions of 2 Gy (day 0 to day +4) or (*B*) two fractions of 6 Gy (day 0 to day +1); data are expressed as percentage of the initial tumor diameters ($n = 8$–11). *C,* for the 2 × (6Gy+BQ123) condition, three doses of BQ123 were tested (0.5, 1, and 2 mg/kg), and mean tumor doubling times were determined (**, $P < 0.01$; $n = 6$–8). Of note, the beneficial effect of the 2 mg/kg dose is underestimated because the doubling time was not determined for 2 mice (of 6), which were in complete remission 5 weeks after the initiation of treatment. BQ123 alone (at each dose tested) failed to produce any significant delay in tumor growth. When coadministered with radiotherapy, BQ123 (or vehicle) was delivered i.p. 45 min before each irradiation; *bars,* ±SD.

of an ET_A antagonist can selectively promote tumor perfusion and oxygenation, and consecutively increase the effectiveness of tumor radiotherapy.

The existence of a myogenic tone is almost impossible to quantitatively appreciate *in vivo,* because it requires the tracking of changes in vascular resistance in response to an increase in transmural pressure. Here, we used a unique experimental model specifically dedicated to this purpose, *e.g.,* microdissected tumor vessels mounted in a myograph allowing step increases in pressure. This *ex vivo* mode of detection should not mask the *in vivo* importance of the myogenic tone in the autoregulation of blood flow by arterioles. Indeed, in normal vascular beds, spontaneous (oscillating) and pressure-induced variations in the muscular tone, known as vasomotion (36) and myogenic tone (35, 37), respectively, offer to the tissue circulation the intrinsic ability to maintain a relatively constant blood flow despite variations in blood pressure. In the case of tumors, such autoregulatory mechanisms are very likely to be needed to face the constant remodeling of tumor vascularization. Here, we have identified the implication of ET-1 as a trigger of the myogenic tone of tumor vessels. The signal transduction appears to transit through the smooth muscle-specific ET_A receptor (the abundance of which is increased by 5-fold in tumor arterioles) because BQ123 (a specific ET_A antagonist) completely abrogated the pressure-dependent development of vascular tone by tumor arterioles.

That the implication of the ET-1/ET_A pathway in the development of a myogenic tone is specific of the tumor vascular bed was additionally authenticated by the increase in blood flow observed after treatment with BQ123 in tumors but not in control tissue from the same mouse (see Fig. 4). Interestingly, ET-1 has been shown to exert its vasoconstrictive effects when applied from the adventitial side of the vessels (38, 39), which in the case of ET-1-producing tumors is very likely to account for local (specific) effects. Moreover, we found an increased vascular ET_A expression in tumor arterioles, which is also very likely to contribute to the observed myogenic tone. Exaggerated production of ET-1 has been reported previously to mediate similar increase in myogenic constriction in cerebral arteries exposed to oxidized low-density lipoprotein (40) and arterioles isolated from hypertensive rats (41). Together with our study, these reports indicate that pathological states such as atherosclerosis, hypertension, and tumor growth can transform vessels devoid of myogenic tone in vessels prone to blood flow autoregulation. Of note, the phenotype shift can be considered as yet more dramatic for tumor vessels, because we used vessels with an external diameter of 300 μm, which is higher than the usually accepted diameter for resistance arterioles (<170 μm).

The observed *ex vivo* and *in vivo* vasodilating effects of BQ123 imply that functional smooth muscle cells are the target of this drug in tumor vessels. The presence of smooth muscle cells or mural cells on vessels is viewed as a hallmark of maturation (42), and it is generally accepted that month/year-old human tumors are more likely to recruit pericytes on a larger proportion of their vasculature (*versus* rapidly growing mouse tumors). This suggests that functional tumor vessels constitute a yet more attractive target for selective vasomodulatory treatments in humans. Although additional studies are required to evaluate how our data can be extrapolated in the clinics, the tumor vessel selectivity of ET_A antagonist treatment, as identified in mouse, offers strong bases for the establishment of an adjuvant strategy aiming to increase the effectiveness of conventional antitumor treat-

Table 1 *Mean regrowth delays for TLT[a] tumors as a function of ionizing radiation exposure(s) and BQ123 treatment(s)*

When indicated (+), BQ123 was delivered i.p. 45 min before each irradiation (2 or 6 Gy) or sham-irradiation (0 Gy).

BQ123 (1 mg/kg)	X-rays (# fraction × dose)	Tumor doubling time (days)	Mean regrowth delay (days)	Mice (*n*)
−	0	4.1 ± 0.7	−	11
−	5 × 2 Gy	8.5 ± 0.6	4.4 ± 0.8	11
+	5 × 0 Gy	4.6 ± 0.3	0.5 ± 0.7	11
+	5 × 2 Gy	13.6 ± 0.7	9.5 ± 0.8	11
−	2 × 6 Gy	13.2 ± 0.9	9.1 ± 0.9[b]	11
+	2 × 0 Gy	4.6 ± 0.4	0.5 ± 0.8	11
+	2 × 6 Gy	23.0 ± 1.4	18.9 ± 0.8[b]	8

[a] TLT, transplantable liver tumor.
[b] $P < 0.01$, *versus* additive effects of BQ123 and X-ray administered separately.

ments (by acting on tumor blood flow and oxygenation). Adequately scheduled combination of these latter approaches with antiangiogenic drugs certainly represents a very attractive area of investigation for future cancer therapy development.

In this study, we provide evidence that acute administration of BQ123 (*i.e.,* i.p. injection 45 min before local tumor irradiation) exerts profound effects on the efficacy of low-dose radiotherapy (5×2 Gy and 2×6 Gy). Importantly, these effects were shown to be ET_A antagonist dose-dependent and obtained using clinically relevant schemes of fractionated radiation administration; a complete remission was even obtained in mice treated with the highest BQ123 dose tested in this study. Although a small effect of BQ123 alone was observed in the absence of irradiation (probably attributable to the antiproliferative effect of this drug; Refs. 27–29), the combination of both irradiation and the ET_A antagonist led to a synergistic effect in both irradiation protocols, increasing the tumor regrowth delay by >50% over the additive effects (see Table 1). We additionally documented that the radiosensitizing effects of BQ123 were very likely to arise from the increase in tumor oxygenation directly associated with the elevation in tumor blood flow (see Fig. 4).

The growing amounts of reports documenting the increase in ET-1 expression in various human tumors (reviewed in Ref. 29) indicate that this approach of blocking the ET_A receptor opens very interesting perspectives in the treatment of many tumor types. Moreover, although we have here only documented the impact of modulating the ET-1/ET_A transduction pathway for radiotherapy, it can be postulated that chemotherapy could also take advantage of a better tumor perfusion and drug delivery. Importantly, this study also confirmed the potential of the myograph assay to identify the existence of a differential reactivity in arterioles issued from animal tumors characterized by different environments (see also Refs. 15, 33). This *ex vivo* pharmacological evaluation of tumor vessels could easily be extended to vessels isolated from human tumor biopsies, and thereby could lead to new insights on "provascular" adjuvant treatments susceptible to improve conventional anticancer treatments.

ACKNOWLEDGMENTS

We thank Delphine De Mulder for excellent technical assistance and Dr. Christine Baudelet for help in the statistical analysis of our data.

REFERENCES

1. Keshet E, Ben Sasson SA. Anticancer drug targets: approaching angiogenesis. J Clin Investig 1999;104:1497–501.
2. Carmeliet P, Jain RK. Angiogenesis in cancer and other diseases. Nature 2000;407: 249–57.
3. Thorpe PE, Chaplin DJ, Blakey DC. The first international conference on vascular targeting: meeting overview. Cancer Res 2003;63:1144–7.
4. Bloemendal HJ, Logtenberg T, Voest EE. New strategies in anti-vascular cancer therapy. Eur J Clin Investig 1999;29:802–9.
5. Jain RK. Normalizing tumor vasculature with anti-angiogenic therapy: a new paradigm for combination therapy. Nat Med 2001;7:987–9.
6. Chaplin DJ, Hill SA, Bell KM, Tozer GM. Modification of tumor blood flow: current status and future directions. Semin Radiat Oncol 1998;8:151–63.
7. Hirst DG, Hirst VK, Shaffi KM, Prise VE, Joiner B. The influence of vasoactive agents on the perfusion of tumours growing in three sites in the mouse. Int J Radiat Biol 1991;60:211–8.
8. Jain RK. Delivery of molecular and cellular medicine to solid tumors. Adv Drug Deliv Rev 2001;46:149–68.
9. Chaplin DJ, Dougherty GJ. Tumour vasculature as a target for cancer therapy. Br J Cancer 1999;80 (Suppl 1):57–64.
10. Jordan BF, Misson P, Demeure R, Baudelet C, Beghein N, Gallez B. Changes in tumor oxygenation/perfusion induced by the no donor, isosorbide dinitrate, in comparison with carbogen: monitoring by EPR and MRI. Int J Radiat Oncol Biol Phys 2000;48:565–70.
11. Fukumura D, Yuan F, Endo M, Jain RK. Role of nitric oxide in tumor microcirculation. Blood flow, vascular permeability, and leukocyte-endothelial interactions. Am J Pathol 1997;150:713–25.
12. Hirst DG, Kennovin GD, Flitney FW. The radiosensitizer nicotinamide inhibits arterial vasoconstriction. Br J Radiol 1994;67:795–9.
13. Emerich DF, Snodgrass P, Dean RL, et al. Bradykinin modulation of tumor vasculature: I. Activation of B2 receptors increases delivery of chemotherapeutic agents into solid peripheral tumors, enhancing their efficacy. J Pharmacol Exp Ther 2001; 296:623–31.
14. Jordan BF, Gregoire V, Demeure RJ, et al. Insulin increases the sensitivity of tumors to irradiation: involvement of an increase in tumor oxygenation mediated by a nitric oxide-dependent decrease of the tumor cells oxygen consumption. Cancer Res 2002; 62:3555–61.
15. Sonveaux P, Dessy C, Brouet A,et al. Modulation of the tumor vasculature functionality by ionizing radiation accounts for tumor radiosensitization and promotes gene delivery. FASEB J 2002;16:1979–81.
16. Griffon-Etienne G, Boucher Y, Brekken C, Suit HD, Jain RK. Taxane-induced apoptosis decompresses blood vessels and lowers interstitial fluid pressure in solid tumors: clinical implications. Cancer Res 1999;59:3776–82.
17. Milas L, Hunter NR, Mason KA, Milross CG, Saito Y, Peters LJ. Role of reoxygenation in induction of enhancement of tumor radioresponse by paclitaxel. Cancer Res 1995;55:3564–8.
18. Bell KM, Prise VE, Chaplin DJ, Wordsworth S, Tozer GM. Vascular response of tumour and normal tissues to endothelin-1 following antagonism of ET(A) and ET(B) receptors in anaesthetised rats. Int J Cancer 1997;73:283–9.
19. Bell KM, Chaplin DJ, Poole BA, Prise VE, Tozer GM. Modification of blood flow in the HSN tumour and normal tissues of the rat by the endothelin ET(B) receptor agonist, IRL 1620. Int J Cancer 1999;80:295–302.
20. Tozer GM, Shaffi KM, Prise VE, Bell KM. Spatial heterogeneity of tumour blood flow modification induced by angiotensin II: relationship to receptor distribution. Int J Cancer 1996;65:658–63.
21. Thews O, Kelleher DK, Vaupel P. Disparate responses of tumour vessels to angiotensin II: tumour volume-dependent effects on perfusion and oxygenation. Br J Cancer 2000;83:225–31.
22. Shankar A, Loizidou M, Burnstock G, Taylor I. Noradrenaline improves the tumour to normal blood flow ratio and drug delivery in a model of liver metastases. Br J Surg 1999;86:453–7.
23. Hahn JS, Braun RD, Dewhirst MW, et al. Stroma-free human hemoglobin A decreases R3230Ac rat mammary adenocarcinoma blood flow and oxygen partial pressure. Radiat Res 1997;147:185–94.
24. Kristensen CA, Roberge S, Jain RK. Effect of tumor necrosis factor alpha on vascular resistance, nitric oxide production, and glucose and oxygen consumption in perfused tissue-isolated human melanoma xenografts. Clin Cancer Res 1997;3:319–24.
25. Liotta LA, Kohn EC. The microenvironment of the tumour-host interface. Nature 2001;411:375–9.
26. Vaupel P, Hockel M. Tumor oxygenation and its relevance to tumor physiology and treatment. Adv Exp Med Biol 2003;510:45–9.
27. Kurbel S, Kurbel B, Kovacic D, et al. Endothelin-secreting tumors and the idea of the pseudoectopic hormone secretion in tumors. Med Hypotheses 1999;52:329–33.
28. Asham E, Shankar A, Loizidou M, et al. Increased endothelin-1 in colorectal cancer and reduction of tumour growth by ET(A) receptor antagonism. Br J Cancer 2001; 85:1759–63.
29. Bagnato A, Spinella F. Emerging role of endothelin-1 in tumor angiogenesis. Trends Endocrinol Metab 2002;14:44–50.
30. Taper HS, Woolley GW, Teller MN, Lardis MP. A new transplantable mouse liver tumor of spontaneous origin. Cancer Res 1966;26:143–8.
31. Bertram JS, Janik P. Establishment of a cloned line of Lewis Lung Carcinoma cells adapted to cell culture. Cancer Lett 1980;11:63–73.
32. Volpe JP, Hunter N, Basic I, Milas L. Metastatic properties of murine sarcomas and carcinomas. I. Positive correlation with lung colonization and lack of correlation with s.c. tumor take Clin Exp Metastasis 1985;3:281–94.
33. Sonveaux P, Brouet A, Havaux X, et alIrradiation-induced angiogenesis through the up-regulation of the nitric oxide pathway: implications for tumor radiotherapy. Cancer Res 2003;63:1012–9.
34. Donckier JE, Michel L, Van Beneden R, Delos M, Havaux X. Increased expression of endothelin-1 and its mitogenic receptor ETA in human papillary thyroid carcinoma. Clin Endocrinol (Oxf) 2003;59:354–60.
35. Davis MJ, Hill MA. Signaling mechanisms underlying the vascular myogenic response. Physiol Rev 1999;79:387–423.
36. Peng H, Matchkov V, Ivarsen A, Aalkjaer C, Nilsson H. Hypothesis for the initiation of vasomotion. Circ Res 2001;88:810–5.
37. Hill MA, Zou H, Potocnik SJ, Meininger GA, Davis MJ. Invited review: arteriolar smooth muscle mechanotransduction: Ca(2+) signaling pathways underlying myogenic reactivity. J Appl Physiol 2001;91:973–83.
38. Pohl U, Busse R. Differential vascular sensitivity to luminally and adventitially applied endothelin-1. J Cardiovasc Pharmacol 1989;13(Suppl 5):S188–90.
39. Mima T, Yanagisawa M, Shigeno T, et al. Endothelin acts in feline and canine cerebral arteries from the adventitial side. Stroke 1989;20:1553–6.
40. Xie H, Bevan JA. Oxidized low-density lipoprotein enhances myogenic tone in the rabbit posterior cerebral artery through the release of endothelin-1. Stroke 1999;30: 2423–9.
41. Huang A, Koller A. Endothelin and prostaglandin H2 enhance arteriolar myogenic tone in hypertension. Hypertension 1997;30:1210–5.
42. Jain RK. Molecular regulation of vessel maturation. Nat Med 2003;9:685–93.